Structures of Tris(donor)-Tris(acceptor)-Substituted Benzenes, 2[1]

Potassium Salts of Trinitrophloroglucinol

J. Jens Wolff*)*, Stephen F. Nelsen*, Douglas R. Powell, and John M. Desper

Department of Chemistry, University of Wisconsin,
1101 University Avenue, Madison, WI 53706, U.S.A.

Received January 14, 1991

Key Words: Conformational analysis / Benzene, donor-acceptor-substituted / Benzene ring, distortion of / Hydrogen bonding, intramolecular / Calculations, AM1

The X-ray crystallographic analysis of the mono-, di-, and tripotassium salts **2b–d** of trinitrophloroglucinol (**2a**) show their benzene rings to become considerably more distorted on successive deprotonation. A parallel increase in C–C, and a decrease in C–O and C–N bond lengths leading to a radialene-type structure is also observed. For **2b**, two chemically different molecules are found in the crystal which differ in their hydrogen-bond pattern as well as in their average bond lengths and deviation of their benzene rings from planarity. AM1 calculations show that for **2b,d** a multitude of structures, differing widely in the deviation of their benzene cores form planarity, can exist within a small energy range (< 3 kcal/mol). The experimental and computational results are discussed in terms of a model that emphasizes "push-pull" interactions as the main cause for the distortions of the benzene rings in compounds of type **1** and **2**.

The benzene ring in triaminotrinitrobenzene derivatives **1b–f** is markedly distorted towards boat[1,2] (**1b–d**) or twist-boat (**1e, f**) forms[1] in the solid state and in solution (Scheme 1). The experimental results and AM1[3] calculations led us to assume[1] that electronic "push-pull" interactions drastically weaken the resistance of the benzene ring towards deformations. Steric interactions and, where possible, hydrogen bonding then determine the actual shape of the benzene core. Nevertheless, a contradiction between theory and experiment remained: all heavy atoms of **1a** are found to be essentially coplanar in the solid state[4], whereas AM1 predicts the benzene ring to be strongly bent into a boat form. Although **1a** may be flat by virtue of the greatly diminished interactions between the substituents in comparison to **1c–f**, and AM1 might therefore just overemphasize the influence of steric contributions to the ring bending, an equally plausible explanation for the planarity of **1a** is offered by its extensive intermolecular hydrogen bonding found in the solid state.

Scheme 1

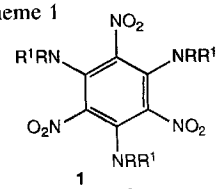

1

1	a	b	c	d	e	f
R	H	Me	Et	*i*-Pr	*neo*-Pentyl	*t*-Bu
R^1	H	Me	Et	H	H	H

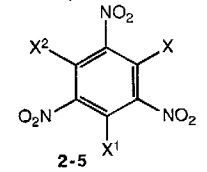

2-5

2	a	b	c	d	3	4	5
X	OH	OK	OK	OK	H	H	H
X^1	OH	OH	OK	OK	H	H	OH
X^2	OH	OH	OH	OK	H	OH	OH

To resolve this discrepancy, we sought molecules that would have donor-acceptor properties similar to **1a** but would have smaller steric interactions and also diminished hydrogen-bonding capabilities. Trinitrophloroglucinol (**2a**) and its mono-, di-, and tripotassium salts[5] **2b–d** fulfill these requirements. A hydroxy group in an *ortho*-nitrophenol will primarily engage in an intramolecular hydrogen bond[6] (see also Scheme 2) which should be easier to model by calculations than intermolecular associations. Although it is also a worse electron donor than an amino group, its deprotonation increases its donor capability considerably while steric interactions are concomitantly decreased. If our hypotheses[1] was correct that donor-acceptor interactions are responsible for the distorted structures of **1b–f**, there should be an increased tendency towards similarly distorted benzene rings in **2** on deprotonation. In this publication, we report on the solid-state structures of **2b–d** and their modeling by AM1 calculations.

Results and Discussion

2b–d were prepared from **2a**[7] by adding the calculated amount[5] of $KHCO_3$; crystals were grown from aqueous solutions and analyzed by X-ray crystallography (Figures 1–5). Selected structural features are shown in Table 1. Two independent molecules are found for **2b** · H_2O, which differ in their pattern of intramolecular hydrogen bonds: $\mathbf{2b_1}$ has both hydroxylic protons bonded to one nitro group (pattern **D** in Scheme 2); in $\mathbf{2b_2}$, they bind to two different nitro groups in a symmetrical fashion (pattern **C**). Both benzene rings are deformed towards a twist boat and show C_2 symmetry. However, there are significant differences in bond lengths and torsional angles. $\mathbf{2b_1}$ has an average C–C bond length that is 0.009(9) Å shorter than that of $\mathbf{2b_2}$ and average

*) New address: Organisch-Chemisches Institut der Universität Heidelberg. Im Neuenheimer Feld 270, W-6900 Heidelberg, F.R.G.

  0009–2940/91/0808–1727 $ 3.50+.25/0

C–N and C–O bond lengths that are longer by 0.005(9) and 0.010(9) Å, respectively (Table 1). We suggest that, based on the observed averaged bond lengths, **2b$_1$** has less of a "push-pull" interaction than **2b$_2$**. It is remarkable to find that its benzene ring is more than twice as much distorted: the sum of absolute values of torsional angles is 18.8(7)° as compared to 8.0(7)°. **2c**, lacking any symmetry (severe disorder is present) was found to be more bent (Table 1) than either form of **2b** and to have longer C–C and shorter C–N bonds. **2d** · 2 H_2O, again C_2-symmetric, continues this trend; its distortion (71°) reaches about half the values of **1e,f**. For this compound, a radialene-type resonance structure acquires considerable weight. Preliminary ^{13}C-NMR experiments[8] on the sodium analog of **2d** indicate that the barrier for conformational interconversion in this compound is comparable to that of **1b–d**.

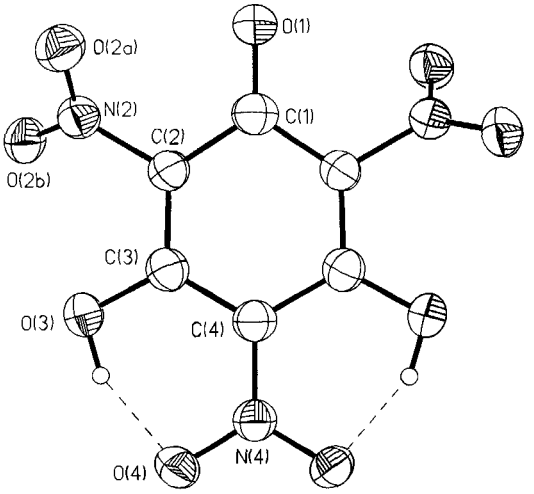

Fig. 1. ORTEP plot of **2b$_1$**

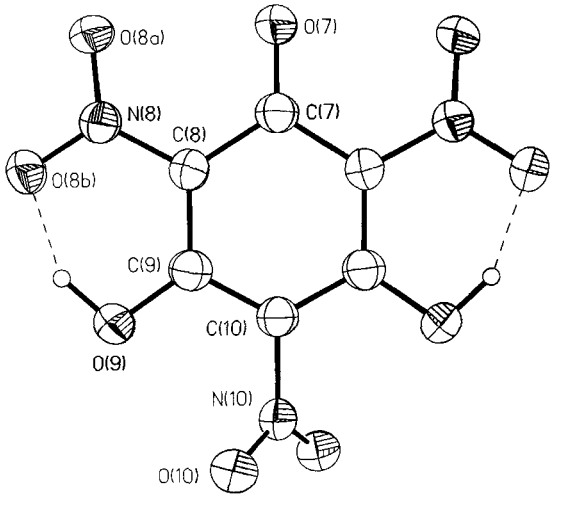

Fig. 2. ORTEP plot of **2b$_2$**

The following generalizations can be made: On going from **2a**[9] to **2d**, the average C–C bond lengths increase substantially, as expected from simple resonance theory. In addition, however, the sums of the absolute values of internal torsional angles are increased dramatically (Table 2). Since structures for a variety of other oxygen-substituted trinitrobenzenes have been reported[9–13], we have compiled the relevant data in Table 2 for comparison. The trends found in this investigation seem general for donor-substituted trinitrobenzenes. Figure 6 is a plot of averaged C–C bond lengths in the benzene core vs. the sum of internal

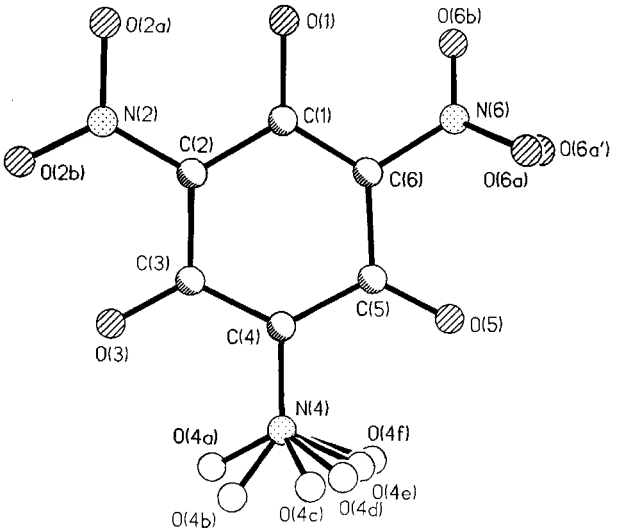

Fig. 3. Ball-stick diagram of **2c**

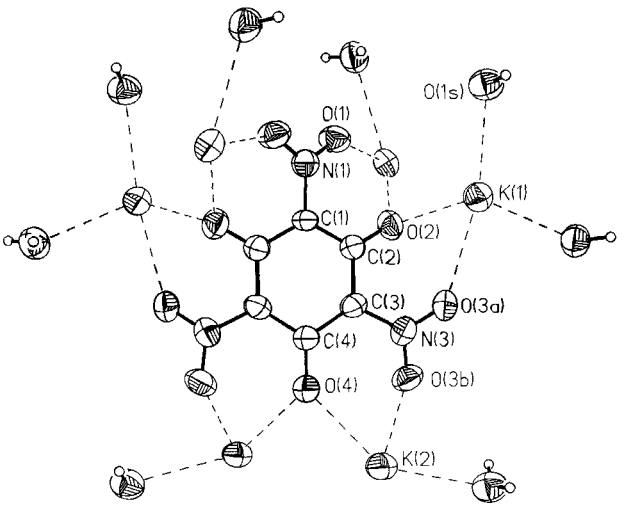

Fig. 4. ORTEP plot of **2d**

torsional angles for compounds **1** and **2**. Although far from excellent, an exponential correlation between bond lengths and sums of torsional angles is definitely present. The only serious exceptions to the general trend observed are found with **1a** and in the comparison of **2b$_1$** to **2b$_2$**, where the latter isomer is less distorted than it should be. We believe that hydrogen bonding is the cause in both cases: In **2b$_1$**, three groups on the benzene core engage in this interaction,

Table 1. Selected structural data for **2b**–**d**

	$2b_1$	$2b_2$	2c	2d
Bond lengths[a] [Å]				
C1-C2	1.438(4)	1.467(4)	1.436(11)	1.436(8)
C2-C3	1.375(5)	1.417(5)	1.491(9)	1.468(7)
C3-C4	1.431(4)	1.387(4)	1.422(12)	1.451(9)
C4-C5	1.431(4)	1.387(4)	1.433(13)	1.451(9)
C5-C6	1.375(5)	1.417(5)	1.476(11)	1.468(7)
C6-C1	1.438(4)	1.467(4)	1.367(11)	1.436(8)
C1-O1	1.249(6)	1.242(6)	1.326(7)	C2-O2 1.249(9)
C3-O3	1.333(4)	1.321(4)	1.249(10)	C4-O4 1.238(9)
C5-O5	1.333(4)	1.321(4)	1.226(11)	C6-O6 1.249(9)
C2-N2	1.455(4)	1.419(4)	1.374(10)	C1-N1 1.410(10)
C4-N4	1.391(6)	1.448(6)	1.435(10)	C3-N3 1.398(10)
C6-N6	1.455(4)	1.419(4)	1.435(12)	C5-N5 1.398(10)
C-C(ave)	1.415	1.424	1.438	1.452
C-O(ave)	1.305	1.295	1.267	1.245
C-NO_2 (ave)	1.434	1.429	1.415	1.402
Nonbonded Distances [Å]				
H1-O2a	-	-	1.383	
H3-O2b	-	1.598	-	
H3-O4	1.666	-	-	
O3-O2b	-	2.481	-	
O3-O4	2.502	-	-	
Torsional Angles [deg]				
C1C2C3C4	4.7(5)	1.5(4)	4.3(9)	17.8(8)
C2C3C4C5	-2.2(2)	-0.7(2)	-1.6(10)	-9.4(4)
C3C4C5C6	-2.2(2)	-0.7(2)	-4.0(10)	-9.4(4)
C4C5C6C1	4.7(5)	1.5(4)	7.8(10)	17.8(8)
C5C6C1C2	-2.5(2)	-0.8(2)	-5.4(10)	-8.2(4)
C6C1C2C3	-2.5(2)	-0.8(2)	-1.0(9)	-8.2(4)
Σ|dih.∠|	19	8	24	71

[a] To achieve consistent numbering, carbon atoms are labeled from 1–6 in all cases, disregarding symmetry. Carbon atoms 1–4 are defined by the X-ray numbering, except for $2b_2$, where carbon atom 7 in the X-ray numbering becomes carbon atom 1 in this table.

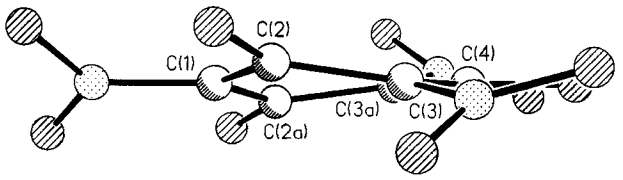

Fig. 5. Edge-on view of **2d**

Scheme 2

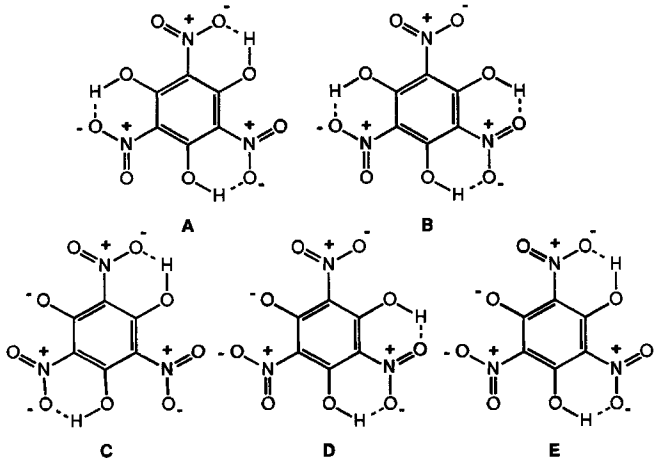

but four in $2b_2$, thus enforcing planarity. **1a**, in addition to the intramolecular interactions between all groups, engages in strong intermolecular interactions. However, it is quite clear that only marginal steric interactions are necessary to cause severe distortions of the benzene core, provided there is strong push-pull interaction as defined by averaged bond lengths. These findings strongly support our analysis[1] of the origins of distortions encountered in compounds of type **1**.

Table 2. Structural features of oxy-substituted 1,3,5-trinitrobenzenes[a]

		3	4	5	2
neutral	C-C(ave)	1.380	1.382	1.388	1.404
	C-N(ave)	1.480	1.462	1.460	1.446
	Σ|dih.∠|	5	5	8	8
mono-	C-C(ave)	-	1.404	-	1.415/1.424
anion	C-N(ave)	-	1.452	-	1.434/1.429
	Σ|dih.∠|	-	8	-	19/8
di-	C-C(ave)	-	-	1.418	1.438
anion	C-N(ave)	-	-	1.436	1.415
	Σ|dih.∠|	-	-	42	24
tri-	C-C(ave)	-	-	-	1.452
anion	C-N(ave)	-	-	-	1.402
	Σ|dih.∠|	-	-	-	71

[a] Potassium as counter ion for charged species, 5^{2-} is a barium salt.

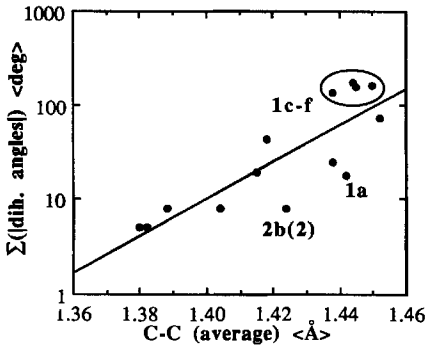

Figure 6. Averaged C–C bond lengths vs. distortions in 2,4,6-tridonor-substituted 1,3,5-trinitrobenzenes

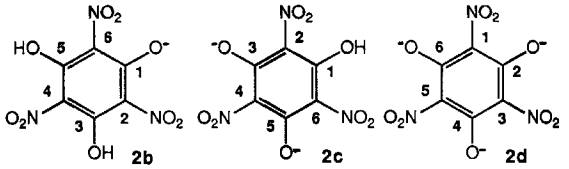

We were interested in comparing the X-ray-crystallographic structures to predictions made by AM1 calculations, especially since the experimental structure for **1a** differs substantially from the calculated one. Crucial to the validity of calculations on systems like **1** or **2** is their capability to reproduce hydrogen bonding. Although earlier semiempirical methods have failed to do so[14], AM1 has been shown to be better in this respect[15], and a report on a successful treatment of intermolecular hydrogen bonding in nitroanilines has appeared[16]. We therefore assumed that, in the case of **1a**, AM1 correctly calculates steric interactions and *intramolecular* hydrogen bonding in the isolated molecule and that *intermolecular* interactions are responsible for the structure observed experimentally. We hoped that this conclusion would be substantiated: AM1 calculations have been performed for **2a**, **b**, **d**, taking into account all possible intramolecular hydrogen-bond patterns. **2a** is calculated to be nearly planar in both **A**- and **B**-type structures (Scheme 2); **A**, optimized with C_3 symmetry, is more stable than **B** (with

C_1 symmetry) by 1.7 kcal/mol. The crystal structure available[9] for **2a** is for a 2/3 hydrate which has pattern **B** with the internally noninteracting nitro group twisted and externally hydrogen-bonded to the water of crystallization. For **2b**, patterns **C**–**E** (Scheme 2) are possible which have been optimized without inclusion of a counter ion. The two most stable structures adopt a boat form: **C**, optimized in C_s symmetry and **E**, which lies 0.6 kcal/mol higher in energy. **D** optimizes 1.7 kcal/mol higher in a C_1 form with an essentially planar benzene ring. However, a careful search of the potential energy surface of pattern **C** revealed that within a range of 0.6 kcal/mol, there are at least four more forms which have drastically different distortions: The sum of absolute values of torsional angles in the benzene ring range form 0.7° to 75.6°. Clearly, a manifold of structures, whose geometries differ substantially from each other, is available within a very small energy range. The structure found experimentally is therefore most likely to be determined by factors that are not included in the calculations (counter ions, water of crystallization, intermolecular interactions between the substituents). Experimental evidence for the near energetic equality between at least two patterns of hydrogen bonding is provided by the fact that **C** and **D** are found to coexist in a hydrated crystal. It comes as no surprise, that AM1 does not find the structures found in the crystal to be energy minima; starting from these, the amount of twist is reversed in $\mathbf{2b_1}$ and $\mathbf{2b_2}$. The general connection between sum of internal torsional angles and averaged bond lengths, however, is still preserved in most cases.

Table 3. Structure determination summary of **2b**–**d**

	2b	2c	2d
Empirical Formula	$C_6H_2KN_3O_9 \cdot H_2O$	$C_6HK_2N_3O_9$	$C_6K_3N_3O_9 \cdot 2\,H_2O$
Color; Habit	yellow needles	yellow prisms	red needles
Crystal Size [mm]	0.10 x 0.15 x 0.35	0.05 x 0.10 x 0.50	0.10 x 0.10 x 0.40
Crystal System	monoclinic	triclinic	trigonal
Space Group	C2/c	P1	$P3_221$
Unit Cell [Å] *a*	7.324(2)	4.226(2)	9.7960(16)
b	20.386(5)	8.686(5)	9.7960(16)
c	14.046(4)	14.216(8)	11.816(2)
[deg] α	90	76.52(6)	90
β	98.34(2)	82.85(6)	90
γ	90	80.98(5)	120
Volume [Å^3]	2075.0(10)	499.1(5)	982.0(3)
Z	8	2	3
Formula Weight	317.2	337.3	411.4
Density (calcd.) [g·cm^{-3}]	2.031	2.245	2.087
Absorption Coeff. [mm^{-1}]	5.233	1.001	10.125
F(000)	1280	336	618
Radiation	CuK_α	MoK_α	CuK_α
Temperature [°C]	-165(2)	-165(2)	19(2)
2θ Range	3.5-114.0°	3.5-50.0°	3.5-114.0°
Reflections collected	1936	2414	2823
Indep. Reflections	1401 (R_{int} = 3.20%)	1743 (R_{int} = 2.48%)	891(R_{int} = 11.45%)
Obsvd. Reflections[a]	1238	1088	818
Absorption Corr.	Semi-empirical	Face-indexed numer.	Semi-empirical
Min/max Transmiss.	0.0531/0.1916	0.8985/0.9490	0.0626/0.4728
Extinction Corr.[b]	χ: 0.0030(4) x: 0.002	N/A	χ: 0.040(4) x: 0.002
Hydrogen Atoms	Located on Difference Map	Riding Model Isotropic U	Riding Model Isotropic U
Weighting Scheme[c]	y = 0.0014	0.0002	0.0016
Parameters refined	189	186	108
Final *R* indices [%] (obsd. data)	R = 3.63 R_w = 5.72	R = 6.76 R_w = 5.94	R = 5.05 R_w = 6.84
R indices [%] (all data)	R = 4.15 R_w = 5.96	R = 11.21 R_w = 6.42	R = 5.48 R_w = 7.07
Goodness-of-fit	1.26	2.06	1.01

[a] $[F > 4.0 \cdot \sigma(F)]$. – [b] $F^* = F(1 + x \cdot \chi F^2/\sin 2\Theta)^{-1/4}$. – [c] $w^{-1} = \sigma^2(F) + y \cdot F^2$.

For the trianion of **2d**, again, a multitude of structures was calculated to exist within a small energy range. A C_s boat, and a C_2 twist-boat structure were found to be stablest (within 0.004 kcal/mol), with an essentially planar structure lying 2.5 kcal/mol above it.

Conclusion

By X-ray analysis, we have shown that successive deprotonation of trinitrophloroglucinol (**2a**) leads to a quite substantial increase in the distortion of the benzene core towards a twist-boat geometry which is associated with an increased [6]radialene character. For **2b**, we have further demonstrated a notable influence of the intramolecular hydrogen-bond pattern on its structural features. AM1 calculations on **2a**–**d** yield a multitude of energy minima within a small energy range, with highly distorted and nearly planar structures separated by barries well below kT, thus demonstrating a very shallow potential surface for the bending of the ring. Taken together, these results clearly support our hypothesis concerning the origins of the large distortions found in 2,4,6-tridonor-substituted 1,3,5-trinitrobenzenes[1]: "push-pull" interactions drastically weaken the resistance of the benzene ring towards bending, and energetically marginal factors, like small steric interactions or hydrogen bonding, determine the actual shape of the molecule.

Table 4. Atomic coordinates ($\times 10^4$) and equivalent isotropic displacement coefficients ($\times 10^3$) [Å] for **2b**; U(eq) defined as one third of the trace of the orthogonalized U_{ij} tensor; O(1W): oxygen atom of water

	x	y	z	U(eq)
K(1)	1618(1)	2801(1)	6560(1)	41(1)
C(1)	0	-1171(2)	2500	40(2)
C(2)	-454(4)	-787(2)	1640(2)	37(1)
C(3)	-530(4)	-113(2)	1622(2)	39(1)
C(4)	0	240(2)	2500	38(2)
O(1)	0	-1784(2)	2500	45(1)
N(2)	-860(4)	-1146(1)	739(2)	39(1)
O(2A)	260(3)	-1558(1)	551(2)	47(1)
O(2B)	-2293(3)	-1020(1)	197(2)	45(1)
O(3)	-1045(3)	199(1)	792(2)	41(1)
N(4)	0	922(2)	2500	38(1)
O(4)	-424(3)	1239(1)	1728(2)	42(1)
C(7)	0	3419(2)	2500	38(2)
C(8)	393(4)	3807(2)	3386(2)	37(1)
C(9)	409(4)	4502(2)	3374(3)	37(1)
C(10)	0	4825(2)	2500	36(2)
O(7)	0	2811(2)	2500	48(1)
N(8)	786(4)	3479(1)	4283(2)	38(1)
O(8A)	677(3)	2879(1)	4358(2)	43(1)
O(8B)	1246(3)	3817(1)	5036(2)	43(1)
O(9)	815(3)	4871(1)	4149(2)	43(1)
N(10)	0	5536(2)	2500	36(1)
O(10)	-1026(3)	5822(1)	2982(2)	43(1)
O(1W)	2123(3)	2947(1)	8620(2)	47(1)

This work was supported in part by the *National Institutes of Health* under GM.29549 J. J. W. thanks the *Humboldt-Stiftung* for a Feodor Lynen fellowship.

Experimental

Potassium Salts of Trinitrophloroglucinol (**2a**)[5]: **2a**[7] [for **2b**: 2.67 g (10.2 mmol); for **2c**: 1.52 g (5.83 mmol); for **2d**: 2.61 g (10.0 mmol)] was dissolved in water (ca. 50 ml), and solid $KHCO_3$ [for **2b**: 1.10 g (11.0 mmol); for **2c**: 2.67 g (11.2 mmol); for **2d**: 3.50 g

(35.0 mmol)] was added. The mixture was heated to boiling for 5 min and was then allowed to cool slowly. **2b–d** were obtained as yellow, orange-yellow, and orange-red needles, respectively.

Table 5. Atomic coordinates ($\times 10^4$), equivalent isotropic displacement coefficients ($\times 10^3$) [Å^2], and occupancies for **2c**; U(eq) defined as one third of the trace of the orthogonalized U_{ij} tensor:

	x	y	z	U(eq)	occ
K(1)	-3068(3)	-3435(2)	8770(2)	48(1)	
K(2A)	625(9)	7034(4)	5317(3)	42(1)	0.525(3)
K(2B)	-960(10)	7692(5)	5375(3)	42(1)	0.475(3)
C(1)	190(14)	912(7)	8188(6)	42(2)	
O(1)	-1733(10)	-176(5)	8598(3)	41(1)	
C(2)	452(14)	2199(7)	8638(6)	45(2)	
N(2)	-1369(11)	2324(6)	9494(5)	44(2)	
O(2A)	-3288(9)	1269(5)	9876(4)	45(1)	
O(2B)	-1344(9)	3408(5)	9919(4)	49(1)	
C(3)	2573(14)	3438(7)	8170(6)	47(2)	
O(3)	2908(10)	4506(5)	8591(4)	59(1)	
C(4)	4084(16)	3309(9)	7235(6)	62(2)	
N(4)	5866(15)	4571(8)	6713(5)	73(2)	
O(4A)	7014(14)	5365(7)	7186(5)	33(1)	0.672(3)
O(4B)	5673(26)	5930(12)	6691(12)	33(1)	0.264(3)
O(4C)	4725(26)	5489(15)	6032(9)	33(1)	0.262(3)
O(4D)	5363(26)	5047(16)	5870(7)	33(1)	0.276(3)
O(4E)	6985(29)	4456(20)	5900(9)	33(1)	0.205(3)
O(4F)	8821(23)	3914(14)	5957(10)	33(1)	0.321(3)
C(5)	3773(17)	2085(10)	6742(6)	75(2)	
O(5)	4928(18)	8018(9)	4065(5)	132(2)	
C(6)	1873(16)	837(9)	7311(6)	55(2)	
N(6)	1646(14)	-480(8)	6884(5)	61(2)	
O(6A)	615(20)	65(11)	5996(8)	48(2)	0.478(3)
O(6B)	1622(12)	-1824(6)	7406(4)	59(2)	

Table 6. Atomic coordinates ($\times 10^4$) and equivalent isotropic displacement coefficients ($\times 10^3$) [Å^2] for **2d**; U(eq) defined as one third of the trace of the orthogonalized U_{ij} tensor; O(1S): Oxygen atom of solvent (water)

	x	y	z	U(eq)
K(1)	5512(2)	10000	1667	57(1)
K(2)	13540(1)	15115(2)	1438(1)	55(1)
C(1)	8298(8)	8298(8)	0	44(3)
N(1)	6859(7)	6859(7)	0	48(3)
O(1)	5643(5)	6759(5)	-407(4)	61(2)
C(2)	8240(7)	9733(7)	-40(5)	46(2)
O(2)	7012(5)	9793(5)	-205(3)	55(2)
C(3)	9758(7)	11183(7)	123(5)	47(3)
N(3)	9694(6)	12532(5)	421(4)	50(2)
O(3A)	8537(5)	12390(5)	960(3)	58(2)
O(3B)	10774(5)	13880(4)	170(4)	59(2)
C(4)	11276(8)	11276(8)	0	46(3)
O(4)	12541(6)	12541(6)	0	65(3)
O(1S)	2509(5)	7413(5)	1460(4)	67(2)

X-ray Analyses on **2b–d**: X-ray data collection: Siemens P3f diffractometer, highly oriented graphite crystal monochromator; scan type: Wyckoff; scan speed: variable, 2.00–12.00° min^{-1} in ω; scan range (ω): 0.40°; background measurement: stationary crystal and stationary counter at beginning and end of scan, each for 16.7% of total scan time. Solution and refinement: Siemens SHELXTL PLUS (VMS)[17], direct methods, refinement by full-matrix least squares. R values for **2c** are high because of severe disorder in the crystal. Further parameters are listed in Table 3[18], atomic coordinates and equivalent isotropic displacement coefficients in Tables 4–6.

CAS Registry Numbers

2b: 133399-90-3 / **2c**: 133399-91-4 / **2d**: 133399-92-5

[1] Part 1: J. J. Wolff, S. F. Nelsen, P. A. Petillo, D. R. Powell, *Chem. Ber.* **124** (1991) 1719, preceding paper.
[2] J. M. Chance, B. Kahr, A. B. Buda, J. S. Siegel, *J. Am. Chem. Soc.* **111** (1989) 5940.
[3] M. J. S. Dewar, E. G. Zoebisch, E. F. Healy, J. J. P. Stewart, *J. Am. Chem. Soc.* **107** (1985) 3902.
[4] H. H. Cady, A. C. Larson, *Acta Crystallogr.* **18** (1965) 485.
[5] R. Benedikt, *Ber. Dtsch. Chem. Ges.* **11** (1878) 1374.
[6] M. C. Etter, *Acc. Chem. Res.* **23** (1990) 120.
[7] J. J. Wolff, H.-H. Limbach, *Liebigs Ann. Chem.* **1991**, 691.
[8] J. J. Wolff, P. A. Petillo, unpubished results.
[9] M. A. Pierce-Butler, *Acta Crystallogr., Sect. B*, **38** (1982) 3097.
[10] C. S. Choi, J. E. Abel, *Acta Crystallogr., Sect B*, **28** (1972) 193.
[11] E. N. Duesler, J. H. Engelmann, D. Y. Curtin, I. C. Paul, *Cryst. Struct. Commun.* **7** (1978) 449; M. Soriano-Garcia, T. Srikishnan, R. Parthasarathy, *Acta Crystallogr., Sect. A.*, **34** (1978) S 114; T. Srikishnan, M. Soriano-Garcia, R. Parthasarathy, *Z. Kristallogr.* **151** (1980) 317.
[12] K. Maartmann-Moe, *Acta Crystallogr., Sect. B*, **25** (1969) 1452; G. J. Palenik, *ibid.* **28** (1972) 1633.
[13] D. Zu-Yue, *Acta Crystallogr., Sect. B*, **38** (1982) 3095; M. A. Pierce-Butler, *ibid.* **38** (1982) 3097.
[14] J. Koller, V. Harb, M. Hodošček, D. Hadžu, *J. Mol. Struct.* **122** (1985) 343 and references therein.
[15] O. N. Ventura, E. L. Coitiño, A. Lledós, J. Bertrán, *J. Mol. Struct.* **187** (1989) 55.
[16] L. K. Vinson, J. J. Dannenberg, *J. Am. Chem. Soc.* **111** (1989) 2777.
[17] G. M. Sheldrick, *SHEXTL PLUS*, Version 4.1, Siemens Analytical X-ray Instruments, Madison, Wisconsin, U. S. A.
[18] Further details of the crystal structure investigations are available on request from the Fachinformationszentrum Karlsruhe, Gesellschaft für wissenschaftlich-technische Information mbH, D-7514 Eggenstein-Leopoldshafen 2, on quoting the depository numbers CSD-320207 (**2d**), CSD-320208 (**2b**), CSD-320212 (**2c**), the names of the authors, and the journal citation.

[31/91]